Pertanika J. Sci. & Technol. 28 (1): 327 - 351 (2020)

PERTANIKA JOURNALS

SCIENCE & TECHNOLOGY

Journal homepage: http://www.pertanika.upm.edu.my/

Review Article

Light Fishing Fleets Monitoring by GIS-Based Spatiotemporal Analysis in West Sumatera Waters

Nurholis[1,2]*, Jonson Lumban-Gaol[2] and Fachrudin Syah Achmad[3]

[1]Graduate School of Marine Technology Program, IPB University, Bogor 16680, Indonesia
[2]Department of Marine Science and Technology, IPB University, Bogor 16680, Indonesia
[3]Marine Science Study Program, Faculty of Agriculture, Trunojoyo University, Madura, Indonesia

ABSTRACT

Studies on the spatiotemporal distribution monitoring of light fishing fleets are limited due to extensive study area, data availability, dynamic distributions, limited monitoring technology, and perception of the fishers. This study aims to monitor and estimate the density of light fishing fleets, representing the centre of fishing areas. Using the visible infrared imaging radiometer suite of boat detection data combined with actual fishing data, the pattern of spatiotemporal distribution of light fishing fleets was analysed, displayed with the variations in sea surface temperature and chlorophyll-a concentrations. This study was carried out at west Sumatera waters. The actual fishing data, light fishing fleets data, and environment parameter data were collected in 2014-2018. The calculation of the geographical distribution was carried out using the geographical information system models with four spatial indicators, i.e., central tendency, spatial dispersion, directional dispersion, and directional trends. The results showed various patterns and behaviours on light fishing fleets spatial distribution. We also revealed the spatiotemporal pattern dynamic of the geographic distribution of light fishing fleets in the west Sumatera waters. The distribution pattern was random compared to the sea surface temperature distribution. On the other hand, it was quite centralized

ARTICLE INFO

Article history:
Received: 28 July 2019
Accepted: 4 November 2019
Published: 13 January 2020

E-mail addresses:
kholiserl@gmail.com (Nurholis)
jonson_lumbangaol@yahoo.com (Jonson Lumban-Gaol)
fachrudinsyah@gmail.com (Fachrudin Syah Achmad)
*Corresponding author

ISSN: 0128-7680
e-ISSN: 2231-8526

following the chlorophyll-a concentration. The distribution of light fishing fleets was dominant in the area with high chlorophyll-a concentration.

Keywords: CFAs, light fishing fleets, spatial indicators, spatiotemporal analysis

INTRODUCTION

Monitoring and mapping of fishing activities are the critical components in the planning and management of fisheries and marine resources (Booth, 2000). Fishing location data have been used for a long time to identify and delineate fishing areas (Jennings & Lee, 2012), assisting the fisheries resource assessments (Booth 2000; Tidd et al., 2017), estimating the fishing efforts (Parnell et al., 2010) and evaluating the impact of external factor interventions in marine and fisheries resource management (Cabral et al., 2016). However, the monitoring and mapping of the fishing activities still face many problems in Indonesia, such as high cost in fishing data collection, low quality of fishing data, and the perception of fishers about fishing data. Many Southeast Asian countries have high fishing densities (*N* boat km^{-2}) (Stewart et al., 2010), while the majority of their fishing fleets have not been equipped with a vessel monitoring system (VMS) (Kroodsma et al., 2018)

Night-time satellite imagery provides an alternative source of spatial data in marine and fisheries studies, especially for vessels using lights as fish aggregating devices (FADs) to attract fish (Kroodsma et al., 2018). Elvidge et al. (2015) stated the potential of VBD (VIIRS Boat Detection) as the boat location extracted from visible infrared imaging radiometer suite, day/night band (VIIRS DNB) image data to provide an advance solution of vessel monitoring activities. The light intensity used in this fishing method allows it to be identified through the night-time image (Geronimo et al., 2018).

Various studies can be carried out by utilizing night-time imaging data such as light pollution mapping in marine protected areas (MPA) (Davies et al., 2014; Davies et al., 2016), offshore drilling mapping (Elvidge et al., 2009; Elvidge et al., 2016), vessel detection and monitoring (Elvidge et al., 2015; Straka et al., 2015), the suitability of fish resource habitats mapping (Kiyofuji & Saitoh, 2004), estimation of fishing effort and intensity for single fish species (Saitoh et al., 2010), and mapping predictions of potential fishing zones (PFZs) (Kiyofuji & Saitoh, 2004; Saitoh et al., 2010; Syah et al., 2016; Setiawati & Tanaka, 2017; Zhang et al., 2017; Geronimo et al., 2018).

In some studies, the night-time imagery was compared to the VMS data to understand the relationship between the fishing gears and the light intensity of the image better. The highest light intensity associates with squid lift fishing gear and small purse seine pelagic (Geronimo et al., 2018), which subsequently associates with FADs for hand line fishing, boat lift net and set lift net. It assumes that the VBD data can delineate fishing grounds for specific fishing gears. Indirectly, the fleet distribution always connects with the spatial

distribution of fish. The spatial distribution of fish is a complex phenomenon controlled by the interactions between various oceanographic and environmental parameters, such as sea surface temperature (SST), sea surface height (SSH), and chlorophyll-a concentration, monitored remotely using satellites (Syah et al., 2016; Setiawati & Tanaka, 2017; Zainuddin 2011). Furthermore, dissolved oxygen, upwelling, salinity, and current can also influence fish distribution

Geographic information system (GIS) technology is specifically designed to visualize, manipulate, manage, and analyse various reference data to determine relationships, linkages, patterns, and trends, which may not be directly proven by the existing data sources (Fischer & Getis, 2010). Development devices in GIS, such as spatial statistical analysis methods, make the researcher easier to study and understand the variation and exploration process of marine and fisheries resources in the spatiotemporal domains (Pierce et al., 2002).

Many studies have utilized the GIS in fisheries science and fishing fleets monitoring in the management aspects (Pierce et al., 2002; Palenzuela et al., 2004; Riolo 2006; Jayaraman et al., 2013) including marine area and fisheries planning (Dineshbabu et al., 2014), modelling the relationship of environmental parameters and fish distribution (Lan et al., 2013; Lumban-Gaol et al., 2015; Lan et al., 2017; Nurdin et al., 2017). In this study, the GIS-based analysis focused on analysing the light fishing fleets density, the spatiotemporal distribution estimations, and the relationship between environmental parameters and the spatiotemporal distribution of light fishing fleets.

The objectives of this study are: (1) to monitor the light fishing fleets density using VBD and actual fishing data, (2) estimate and observe the pattern of the spatiotemporal distribution of light fishing fleets in the west Sumatera waters (WSW) against SST and chlorophyll-a concentrations. The results are expected to provide information on new approaches for monitoring light fishing fleets and assist the decision makers in managing fisheries resources in WSW.

MATERIAL AND METHODS

Study Area

This research was conducted in the west Sumatera waters (WSW). The WSW is the part of the Republic of Indonesia Fisheries Management Area named WPP RI 572. Characteristically, the WSW is slightly different compared to the South Java Sea (SJS). Upwelling occurs in SJS during the southeast monsoon and also affected by the Indonesian current which flows through Sunda Strait and carries rich nutrients from Java Sea. Our study area is shown in Figure 1.

Fisheries Data

The actual light fishing fleet data were collected from the daily logbook of hand line fishing boats in 2014-2018 within various gross tonnages (GT). The hand line fishing is a simple fishing gear consisting of fishing lines, snap, connectors, and hooks, and generally used for demersal fishery (Mulyadi et al., 2015). The actual fishing fleet data were filtered and selected based on the attributes needed in this study, as shown in Table 1. Furthermore, the data were converted in the GIS software and re-filtered to ensure a clean outliers fishing point. The data were also compiled in GIS software to observe the spatiotemporal distribution. The actual fishing fleet data were overlaid with the VBD density to determine whether VBD data are representative of actual data or not. The aim of overlaying data was to identify the CFAs in the WSW. Flow chart analysis of fishing fleet data can be seen in Figure 2.

Figure 1. Area of Interest (AOI) in West Sumatera Waters (WSW)

Table 1

The actual fishing data used in this study

No	Lon	Lat	(*n*)	(*w*)	(*t*)	day	month	year
1	99.45	-1.26	1	50	38	2	1	2016
2	99.35	-1.32	1	46	49	3	1	2016
3	99.44	-1.42	1	71	49	4	1	2016
4	99.47	-1.46	7	390	49	5	1	2016
No_i	Lon_i	Lat_i	n_i	w_i	t_i	day_i	$month_i$	$year_i$

Note: *n* = total fishing catch, *w* = weight of fishing catch, *t* = fishing trip
Source: Daily logbook datasheet of Bungus Fishing Port

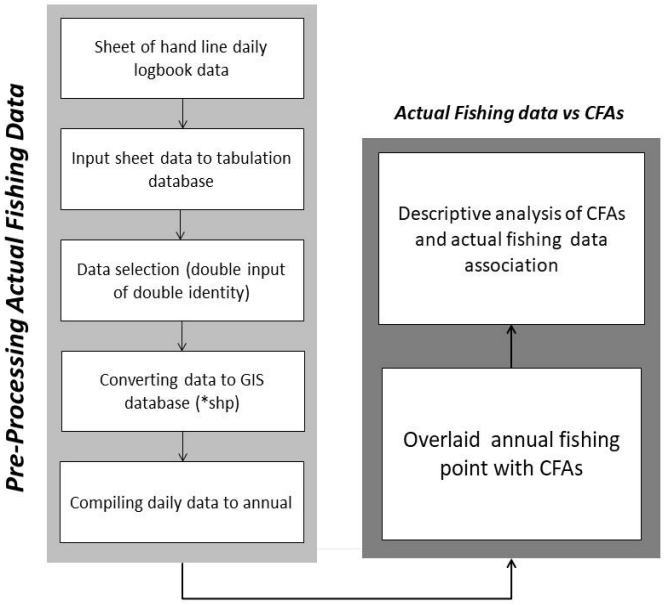

Figure 2. Flowchart of hand line actual fishing data analysis

VIIRS Boat Detection Data

VIIRS is the primary imager on Suomi National Polar Partnership (SNPP) that has been successfully launched in 2011. The VIIRS DNB collects low light imaging data with 45 times smaller pixel footprint than the OLS. One of the initial products of VIIRS DNB is VBD data, known as boat location that detected from present of lights intensity in the ocean (Elvidge et al., 2015). The light fishing fleets data were extracted from the VBD data. Those data were downloaded from the U.S National Oceanic and Atmospheric Administration National Centre for Environmental Information's Earth Observation Group website (www.ngdc. noaa.gov/eog/viirs/downloadphil.boat.html) from 2014 to 2018. Each VBD datum represents pixels which are suspected to be boat lights in the VIIRS DNB image (Elvidge et al., 2015; Cozzolino & Lasta, 2016; Elvidge et al., 2018).

The VBD data files contained information on the ship's suspect pixel geolocation, such as radiances value (nanoWatts/cm^2/sr), date, image acquisition time, image data processing date, and ship detection quality (quality flag) (Geronimo et al., 2018). Each detection quality information is represented by these symbols, QF_1 (strong boat detection), QF_2 (weak boat detection), QF_3 (blurry boat detection), QF_8 (recurring lights) and QF_10 (weak and blurry lights/gas flares) symbols (Elvidge et al., 2015). In this study, only data with QF_1 criteria were used for further analysis to represent ships with high light intensity, undoubtedly related to the number of FADs (Table 2). The data warehousing process was carried out in GIS platform using several toolboxes.

Generally, the procedures were applied for this study is pre-processing VBD data and pattern identification. Pre-processing activity includes conversion, query, and delineation area of interest. We performed "point to raster" tools in the pattern identification stage to create annual VBD presence raster with 700 x 700 m^2 resolution. Kernel density was also performed to identify the light fishing fleets spatial pressure. Based on density information we clustered the density by visual interpretation and manual digitation to identified CFAs. The density clustering process also based on field information of dominant traditional PFZs at study area. CFAs location and identity determined by local spatial knowledge, and then we calculated the total area. To obtain information on the dynamics of the geographical distribution of light fishing fleets we also performed the "spatial statistics tool". Monthly light fishing fleets position data per season then overlaid with spatial analysis results and environmental parameters namely SST and chlorophyll-a concentration. The flow chart for VBD data processing is shown at Figure 3.

Table 2

Dominant fishing gears using light as Fish Aggregating Devices (FADs) in the Western Indian Ocean

No	Fishing Gears	Target Species	Light Description
1	Purse seine	Tuna, Mackerel Tuna, Skipjack, Mackerel	HPIT Spotlights with halogen bulb 1000-5000 watt/ 15-40 bulbs or FADs, depending on the ship size
2	Hand Line	Yellow Fin Tuna, Big Eye Tuna, Demersal Fishes	HPIT Spotlights with halogen bulb 1000-5000 watt/10-20 bulbs or FADs
3	Boat lift net	Skipjack, Mackerel Tuna, Mackerel	HPIT Spotlights with halogen bulb 1000-5000 watt/10-30 bulbs or FADs; sometimes, underwater lights are also used with a capacity of 500-1000 watts/2-8 units or FADs
4	Set lift net	Anchovies, Squid, other little pelagic fish	LED or metal halide bulbs with size 30-100 watt/5-20 bulbs or FADs, sometimes, underwater modified lights are also used.

Source: Statistic report of Bungus Fishing Port (2017) and Geronimo et al. (2018)

Spatiotemporal Analysis of Light Fishing Fleets Distribution Pattern

The calculation of the geographical distribution was carried out using the GIS-based model to determine 4 spatial indicators, namely central tendency, spatial dispersion, directional dispersion, and directional trends (Figure 3) (Fischer & Getis, 2010). GIS based model applied in this study is spatial statistical analysis (Fischer & Getis, 2010; Perzia et al., 2016). It is a well-known spatial modelling because of flexibility in data storage and management, easy to understand both analytical and technical, and applicable. The spatial tendencies

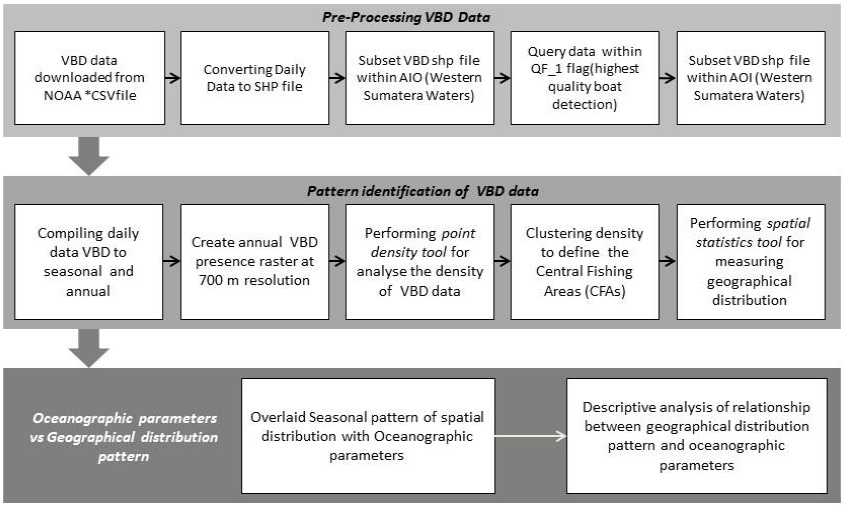

Figure 3. Flowchart of VBD data application to detect spatiotemporal patterns of light fishing fleets distribution in West Sumatera Waters

were calculated using the "mean centre tool" which is the distribution geographical centre calculation of the light fishing fleets, the average *x*, and *y* coordinates of the total VBD coordinates in the study area. Changes in the central tendency reflect variations in the distribution of light fishing fleets both spatially and temporally (Perzia et al., 2016).

The spatial dispersion was calculated using a "standard distance tool" representing the degree where the spatial fishing fleets are spatially concentrated or distributed around the central tendency. The spatial dispersion maps is represented by circles with a radius equal to 95% of the total VBD data as input in the study area. The radius value of the circle was assumed as the concentration level of the spatial distribution. The greater of the circle radius value, the more dispersed the light fishing fleet spatial distribution will be or vice versa (Perzia et al., 2016).

Directional dispersion and directional trend were calculated using the "standard deviational ellipses tool." The directional scattering calculated the standard distance from the direction of the *x* and *y* coordinates distributions that were represented by oval visualization containing 95% of the total data input. Thus, the extent of light fishing fleet distribution in an area was determined. On the other hand, directional trends stated the direction degree of the distribution data input. The directional trends are representations of extending clockwise axis rotation starting at mid-day point. Generally, the description and equations of the spatial indicators that performed in this study is shown in Table 3.

Central tendency was average of total *x* (longitude) and *y* (latitude) coordinates in the study area. Spatial dispersion was the result of standard deviation of total *x* and *y* coordinates over study area, while the directional dispersion was standard deviation over

x coordinates and standard deviation over *y* coordinates that represent of standard distance over the direction of *x* and *y* coordinates. Directional trends were the calculation of degree A, B, and C. Clear brief of this equation explained as follow:

$$A = \left(\sum_{i=1}^{n} \tilde{x}_i^2 - \sum_{i=1}^{n} \tilde{y}_i^2\right) \quad B = \sqrt{\left(\sum_{i=1}^{n} \tilde{x}_i^2 - \sum_{i=1}^{n} \tilde{y}_i^2\right)^2 + 4\left(\sum_{i=1}^{n} \tilde{x}_i\, \tilde{y}_i\right)^2} \quad C = 2\sum_{i=1}^{n} \tilde{x}_i\, \tilde{y}_i$$

$\tilde{x}_i$ and $\tilde{y}_i$ are the deviations for the x-y coordinates from the mean centre calculation.

Table 3

Spatial indicators used in this study

Spatial Indicators	Equations	Spatial Scale	Time Scale	Ecological Explanation
Central Tendency	$\bar{X} = \frac{\sum_{i=1}^{n} xi}{n} \bar{Y} = \frac{\sum_{i=1}^{n} xi}{n}$	Global	Daily & Seasonal	Centre of the fishing fleet
Spatial Dispersion	$SD = \sqrt{\frac{\sum_{i=1}^{n} \left(xi - \bar{X}\right)^2}{n} + \frac{\sum_{i=1}^{n} \left(yi - \bar{Y}\right)^2}{n}}$	Global	Daily & Seasonal	Spatial dispersion Coordinates of light fishing fleets
Directional Dispersion	$SDx = \sqrt{\frac{\sum_{i=1}^{n} \left(xi - \bar{X}\right)^2}{n}}$ $SDy = \sqrt{\frac{\sum_{i=1}^{n} \left(yi - \bar{Y}\right)^2}{n}}$	Global	Daily & Seasonal	Directional distribution of axis *x* and *y*
Directional Trend	$\tan\theta = \frac{A + B}{C}$	Global	Daily & Seasonal	The directional tendency of light fishing fleets (spatial distribution)

Source: (Perzia et al., 2016)

Effect of Environmental Parameters on Fleet Spatial Distribution

The relationship between spatial fish distribution and oceanographic parameters tends to be non-linear (Bertrand et al., 2004; França et al., 2012). Nevertheless, the prediction of PFZs is still carried out based on signs of biophysical conditions in the aquatic environment. It proves that it has a significant contribution to the influence of the fish distribution and fishing fleets distribution. The SST and chlorophyll-a are known as parameters widely used for PFZs analysis (Zainuddin & Saitoh, 2008; Lanz et al., 2009; Nurdin et al., 2017).

The chlorophyll-a can determine water productivity and fish production even though the relationship is not direct (Bertrand et al., 2002). Lumban-Gaol et al. (2015) explained

that the sea level and eddies current indirectly indicated good habitat for the feeding area. The environment data were overlaid with the VBD's geographical distribution to understand the daily and seasonal distribution patterns of the fishing fleet. The daily sample data were taken at the new moon phase in each month (every season) to ensure that the detected activity points have the best radiance intensities (Elvidge et al., 2015). More explanation on the type of data, unit of data, description, and source of data is shown in Table 4.

Table 4

Materials, data units, descriptions and data sources

Data Type	Data Source	Description
Actual Fishing Data		
Actual fishing data	Daily logbook of the hand line fishing	Bungus fishing port daily logbook datasheets
Environmental Data		
Sea Surface Temperature (SST)	http://marine.copernicus.eu/	Monthly; The Global ARMOR3D L4 dataset; data combination AVHRR, AMSR and in situ observation of NCDC NOAA; spatial resolution 0.25°x0.25°
Chlorophyll-a concentration	*http://marine.copernicus.eu/*	Monthly; PISCES biogeochemical model data, spatial resolution 0.25°x0.25°;
Light Fishing Data		
VIIRS Boat Detection	https://www.ngdc.noaa.gov/eog/viirs/download_boat.html	Daily; VBD data (VIIRS Boat Detection) level 3; spatial resolution (0.375 km – 1.6 km); scanning width 3000 km

RESULTS AND DISCUSSION

Figure 4 shows the total fleets detected by VIIRS DNB at the pixel area (700 x 700 m). High value of detected fleet (5 to 36 units per pixel) dominantly were at the coast water of west Sumatera, Mentawai strait, and coast water of Bota Island at the southern part of study area. Low value of detected fleet (1 to 5 units per pixel) dispersed within the study area. This information represented fishing pressure at the study area based on light fishing fleets spatial distribution. Figure 5 shows the DNB radiance value that represents the light intensity detected from DNB Image. Both figures relate to the density of the light fishing activity and the dominant fishing gear types operated at that area. Higher radiance value suspected related to the fishing gear that utilized big amount of lights as FADs (Table 2). The light used at the fishing activities linearly correlated with the radiance value that was detected by VIIRS DNB Image.

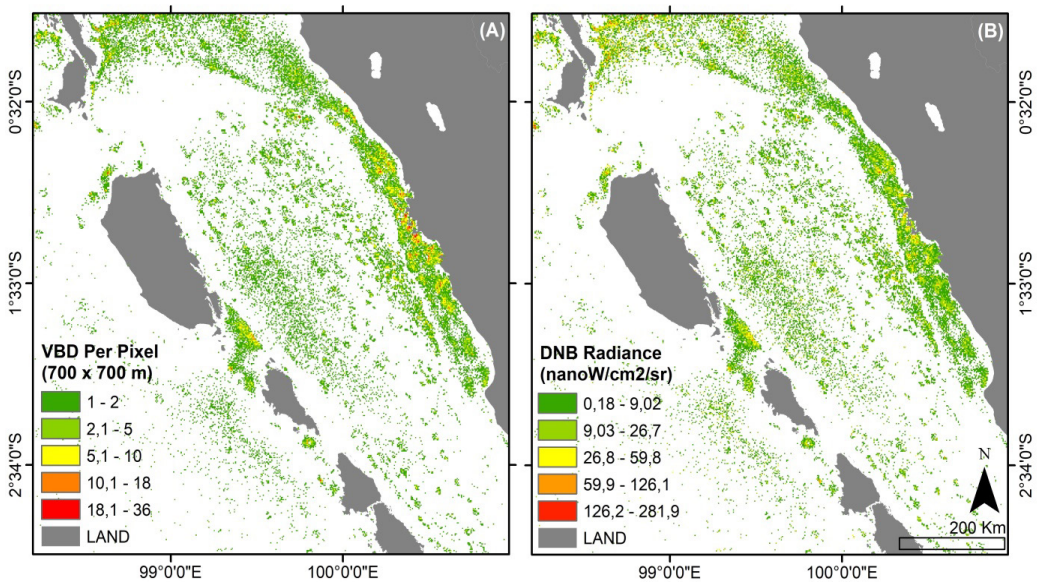

Figure 4. VBD data from 2014 - 2018 were rasterized with a resolution of 700 x 700 m (A) The number of VBD detected per pixel from 1780 nights and (B) Radiance values for each VBD point detected

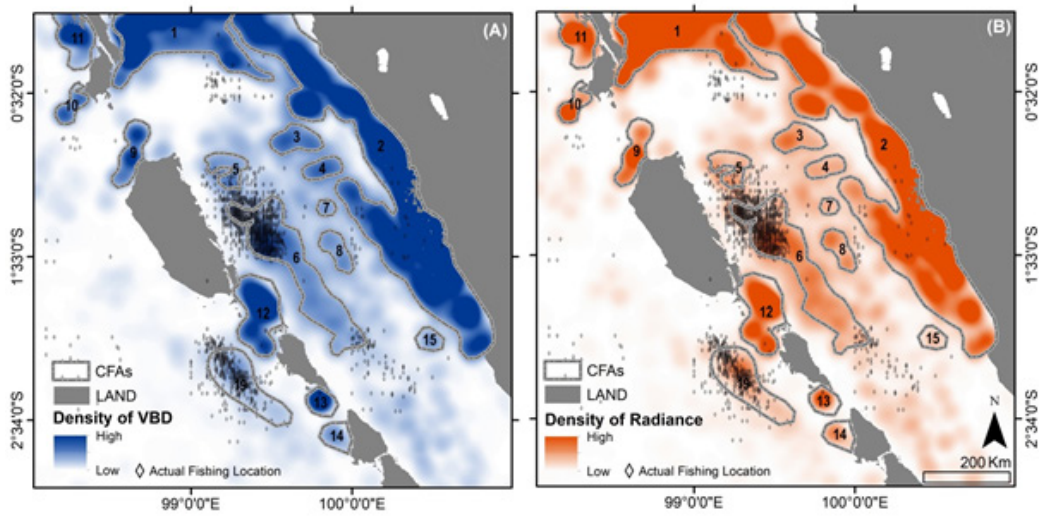

Figure 5. Central Fishing Area (CFA) and actual fishing fleets data in West Sumatera Waters during 2014-2018. (A) CFA and spatial density of the number of VBD/pixel (B) CFA and spatial density of radiance values/pixels

The VBD in WSW indicates a variation in the spatial patterns, i.e., the number of VBD per pixel and radiance value per pixel. The number of VBD per pixel was dominantly seen in classes 1 to 2 VBD, while the class above 2 was dominant at coast waters and Mentawai strait. The dominant radiances have been seen in class that is smaller than 26.71 $nW/cm^2/sr$. The spatial pattern of the high radiances was consistent with the VBD's value per pixel, which tended to be in the coastal water areas (Figure 4).

Figure 4 shows that the spatial pattern of dominant radiance value < 9.03 $nW/cm^2/sr$ spread throughout the area, while the spatial pattern of radiance value > 9.03 $nW/cm^2/sr$ was dominantly located near the coast and straits of the study area. This due to < 10 GT vessels are generally lift net and mini purseseine that densely distributed in the coastal waters of west Sumatera. They predominantly used 5-40 lights as FADs, causing the value of detected radiances intensity greater and clearer in the coastal area. The difference in detected radiances intensity was highly related to the number of lights used in fishing activities (Hsu et al., 2019).

The radiance intensity was expressed in $nW/cm^2/sr$ for the boat detection. Actual radiance intensity data was expressed in $W/cm^2/sr$ that had seven to ten zeros after the decimal point before the start of significant digits. For better understanding, the $W/cm^2/sr$ was multiplied by billion and became $nW/cm^2/sr$. This idea intended to produce number with one or two digits to the left of decimal point and a string of values to the right of the decimal point (Elvidge et al., 2015). High intensity of radiances represents high intensity light sources at sea. The high radiance distribution at coast water of west Sumatra explained that dominant fishing gear used at that area was boat lift net. Boat lift net is light based fishing gear that catches pelagic fish, operates at night and utilizes 30 – 60 light sources. At the center of Mentawai strait, radiance intensity became smaller due to long line, hand line and purse seine fishing activity.

The ability of VIIRS night imaging is very significant in improving the quality of night-time image results compared to its predecessor, the DMSP satellite in terms of radiometric resolution and spatial resolution; that is very important in the process of extracting information on vessel position through lights in the sea (Miller et al., 2013 & Elvidge et al., 2015). Another advantage of using VIIRS DNB data is VIIRS day/night band (DNB) collects low light imaging data 45 times smaller pixel footprint than the DMSP (Elvidge et al., 2013). Elvidge et al. (2015) explained that VIIRS DNB also had higher level of quantization, rigorous calibration, and additional spectral bands useful for cloud, ocean and combustion source characterization. Further, they stated that VIIRS had high capability of detecting vastly more lit fishing boat features when compared to DMSP.

According to all of the advantages of VIIRS DNB data among DMSP, we assessed some fisheries study based on this datasets. VBD data is a new product that produced from VIIRS DNB data analysis. In this study, we performed VBD data to identify, delineate,

characterize and analyse the CFAs in WSW. The CFAs also compared with actual fishing position data to analyse how the CFAs relates to the actual fishing activities within study area.

CFA from VBD Data

The analysis of the VBD data (2014 - 2018) showed spatially different densities. The high-density radiance was more concentrated in coastal areas while low-density VBD numbers covered a wider area. This spatial density informed that the pressure of fishing activities at WSW tended to occur in the waters of the strait and coast (Figure 5). The pattern of the spatial density was used as an excuse to predict the causes of high fishing activities in these locations.

The pattern of spatial density was used as the basis for determining and identifying CFAs in WSW. Besides, it was also used to compare the spatial patterns of CFAs with the actual fishing data. The spatial interpretation was conducted to delineate the location of the CFAs. A total of 19 CFAs was identified in WSW (Figure 5) with varying areas and shapes (Table 5). The widest CFAs was recognized at CFAs No. 2 which reached 9813.74 km^2 in the coastal area of the west coast of west Sumatra. The location of the CFAs extends from the south to the north near the strait of the Islands. The smallest CFAs was identified as CFAs No. 16 covering 29.50 km^2 in the northern coast of North Pagai Island or Pagai waters. It was PFZs for traditional fishers from the north and south Pagai Islands, predominantly using the boat and set lift net. All the extent of CFAs and the identification of each CFAs are shown in Table 5.

The result of CFAs identification and actual data on hand line fishing determined that the actual point of hand line fishing was included in certain CFAs or associated with some CFAs. CFAs No 1, 5, 6, 8, and 19 were the most related CFAs to actual data. The highest intensity of the actual data was at CFAs No 6, which was at range of 99^{o}E - 99.5^{o}E and 1^{o}S - 2^{o}S corresponding to the Mentawai Strait. The intensity of the fishing activities from the actual data was also high at CFAs No. 19, which was west of Sipora Island water. The CFAs data and identification results provided information related to the traditional PFZs at WSW. However, those CFAs intersect with the other conventional PFZs of fishing gear such as lift net, longline and purse seine which were also the dominant fishing gear used by fishers in the WSW (Harahap et al., 2018). Lift net, longline and purse seine PFZs were also used in certain zones around the Mentawai strait in the No.6 CFAs area.

CFAs data also are applied to identify tuna fishing centres, especially hand line fishing. The WPP 572 is also known as traditional PFZs for tuna fishing vessels, coming from Sibolga fishing port at north Sumatra, Bungus fishing port and Nizam Zachman fishing port at Jakarta. WSW is one of strategic traditional PFZs of hand line in west Sumatera in term of accessibility, productivity and connectivity. A traditional PFZs means that the

Table 5

Identification of Core Fishing Area (CFA n = 19) in the West Sumatera Waters

CFAs No	Extensive Estimation (Km^2)	CFAs Description
1	3630.54	Bota Island strait
2	9813.74	West coast waters of West Sumatera
3	507.11	Mentawai strait I
4	307.32	Mentawai strait II
5	433.23	Off the east coast water of Siberut Island I
6	2729.01	Off the east coast water Siberut & Sipora Island
7	118.32	Mentawai strait III
8	380.47	Mentawai strait IV
9	617.64	North coast water of Siberut Island
10	314.89	Southwest coast water of Bota Island
11	921.29	West coast water of Bota Island
12	1276.93	Bunga Laut strait
13	305.86	Sipora strait
14	329.35	South coast water of South Pagai Island
15	226.41	Mentawai strait V
16	129.50	North coast water of North Pagai Island
17	720.20	Off the coast South Pagai Island
18	1082.20	Southern water of Pagai Island
19	1338.26	Western water of Sipora Island

Source: Analysis of VBD and actual fishing data

PFZs is determined by conventional methods, such as fishing habits, natural signs (flying birds, schooling dolphins, ripples on the sea surface) and foreign objects that float in the waters (Nurdin et al., 2010; Nurdin et al., 2015; Nurdin et al., 2017). PFZs is always connected to a fishing base as the pre and post fishing activities base (fishing port) (Hsu et al., 2019). This result is still relevant to explain because fleets detected in the night-time imagery are dominantly catching pelagic fish as well as hand line fishing vessels that catch yellow fin tuna. Yellow fin tuna distributes vertically near to water surface during the night, so it was possible to used lights as FADs for hand line.

Internal and external factors in fishing activities significantly influence the fishing locations base on types of fishing gear in WSW. Thus, the identification results were not representative to describe certain kinds of fishing gear (PFZs). Girardin et al. (2017)

explained similar aspects, where the factors influenced Fisher's decision in choosing fishing locations and also projections of expenditure, estimation of risks, and habits in determining fishing areas. Furthermore, Geronimo et al. (2018) explained that environmental factors had a very high influence on the spatial structure of VBD detection results, especially in locations with high spatial density.

Moreover, the approach used the VBD data which could not distinguish certain types of fishing gear in waters. However, despite these shortcomings, the existence of information regarding the distribution of fishing activities that is openly accessible, made it possible to fill the gaps of data availability that can be used in marine and fisheries management studies (Elvidge et al., 2015; Geronimo et al., 2018).

Geographic Distribution Estimation from VBD Data

Table 6 reveals the results of the estimation of spatial indicators (central tendency, spatial dispersion, directional dispersion, and directional trends) which were estimated from the sample of daily data in 2014-2018. Dataset was selected in the day in the new moon phase to ensure the clearest intensity from ship's lights representing the vessels position (Elvidge et al., 2015). However, there were < 5 units of VBD data detected and causing the estimation of geographical distribution unsuccessful.

The daily VBD unit ranged from 0-200 units during the year. The highest VBD unit was detected in July 23rd, 2017 as many as 174 units (during the day in the southeast monsoon season). The lowest VBD units were 0 units on April 25th, 2017 (during a day in the transition I monsoon). Atmospheric and oceanographic conditions played the main role in determining the VBD unit at sea (Elvidge et al., 2015; Geronimo et al., 2018). The amount of VBD detected daily was very influential on the results of daily geographical distribution estimation per season in 2014-2018. Unsuccessful quantification of geographical distribution was caused by the presence of < 5 unit data at our dataset. The distribution pattern and unsuccessful quantification of geographical distribution are shown at Figure 6.

Generally, the result confirmed that geographic distribution of light fishing fleets was wider during the northwest and southeast monsoon and became more compact at transition I and II monsoon. The variability of SST and chlorophyll-a concentration during different season influenced the geographic distribution of light fishing fleet at west Sumatera waters. Geronimo et al., (2018) reported that environment parameter as the main influence of the light fishing fleet distribution at sea.

Table 6 shows the estimation results of the spatial indicators for the daily data per season in 2014–2018. The highest spatial value of spatial dispersions was identified in the 2016 northwest monsoon with a value of 168.94 km. This value indicates a wider distribution of fishing activities in the study area. The same result was also identified in the spatial

indicator of directional dispersion in the same year for the *x* value of 204.92 km, but the *y* value did not necessarily has linear values that increased against the value of *x* and spatial dispersion. The trend of the direction of distribution monitored from the estimation results showed the geographical orientation in the value range between 97.99°-171.48°. The value of spatial indicators was determined by fishing points dispersion at sea that influenced by oceanographic parameters, fishers skill, fishing season, and accommodation (Kaschner et al., 2006; Saraux et al., 2014; Perzia et al., 2016; Harahap et al., 2018). Furthermore, it can be seen in Table 6 that the fishing activities were more dispersed in the northwest and southeast monsoon, which was confirmed by the visual appearance in Figure 6.

The central tendency of the VBD distribution or fishing activities of the sample days in each season from 2014 to 2018 is shown in Figure 6. The central tendency on the sample day of the transition I and transition II was more spatially dispersed. It shows that some points located slightly far in the south and west. In the central tendency in the northwest and southeast monsoon, the sample data tended to be centred and shifted less in the study area, which is only concentrated at 99°E - 100°E and 0.5°S - 2°S (Figure 6 of mean centre). This is also clearly confirmed by the results of other spatial indicator estimations shown in Figure 6 and Table 6. The daily sample data showed variations in the distribution of the detected fishing activities based on vessel lights. The spatial pattern and estimation results represented the dynamics of fishing activities of the lighted fishing fleet at the WSW.

The GIS approach has been widely applied in marine and fisheries studies, such as Perzia et al. (2016) in terms of monitoring of sword fishing activities and CPUE (Catch per Unit Effort) analysis; fisheries management planning (Close & Hall, 2006); fish pelagic distribution modelling (Saraux et al., 2014 & Harahap et al., 2018); and the relationship between environmental parameters and fish distribution (Kaschner et al., 2006). The GIS enables more dynamic and efficient management (fisheries and marine spatial) of data with the methods that are flexible regarding storage and processing (Perzia et al., 2016). The GIS-based analysis proved that it could be an alternative approach for marine and fisheries resources management.

Table 6

Spatial indicator values of daily geographical distribution per season 2014-2018

Object ID	Seasons	Spatial Dispersion (km)	Directional Dispersion *x* (km)	Directional Dispersion *y* (km)	Directional Trends (°)
1.14	Northwest Monsoon	147.89	160.69	133.86	156.59
1.15	Northwest Monsoon	124.57	160.34	72.99	150.65

Table 6 *(Continued)*

Object ID	Seasons	Spatial Dispersion (km)	Directional Dispersion *x* (km)	Directional Dispersion *y* (km)	Directional Trends (°)
1.16	Northwest Monsoon	168.94	204.92	122.84	109.95
1.17	Northwest Monsoon	110.21	135.07	77.76	123.47
1.18	Northwest Monsoon	104.57	127.86	74.30	132.85
4.14	Transition I	101.69	132.07	56.92	130.09
4.15	Transition I	0.00	0.00	0.00	0.00
4.16	Transition I	127.61	139.84	114.07	157.46
4.17	Transition I	0.00	0.00	0.00	0.00
4.18	Transition I	0.00	0.00	0.00	0.00
7.14	Southeast Monson	160.61	138.95	179.68	70.04
7.15	Southeast Monson	89.29	95.63	82.46	171.48
7.16	Southeast Monson	172.05	216.65	110.76	97.99
7.17	Southeast Monson	102.37	118.52	83.14	127.70
7.18	Southeast Monson	156.57	213.05	60.32	144.10
10.14	Transition II	112.25	122.45	101.03	124.88
10.15	Transition II	0.00	0.00	0.00	0.00
10.16	Transition II	65.15	91.53	10.61	142.63
10.17	Transition II	123.88	160.21	70.89	154.71

Note: Object ID (Month.Year) → (1.14) → (January 2014)

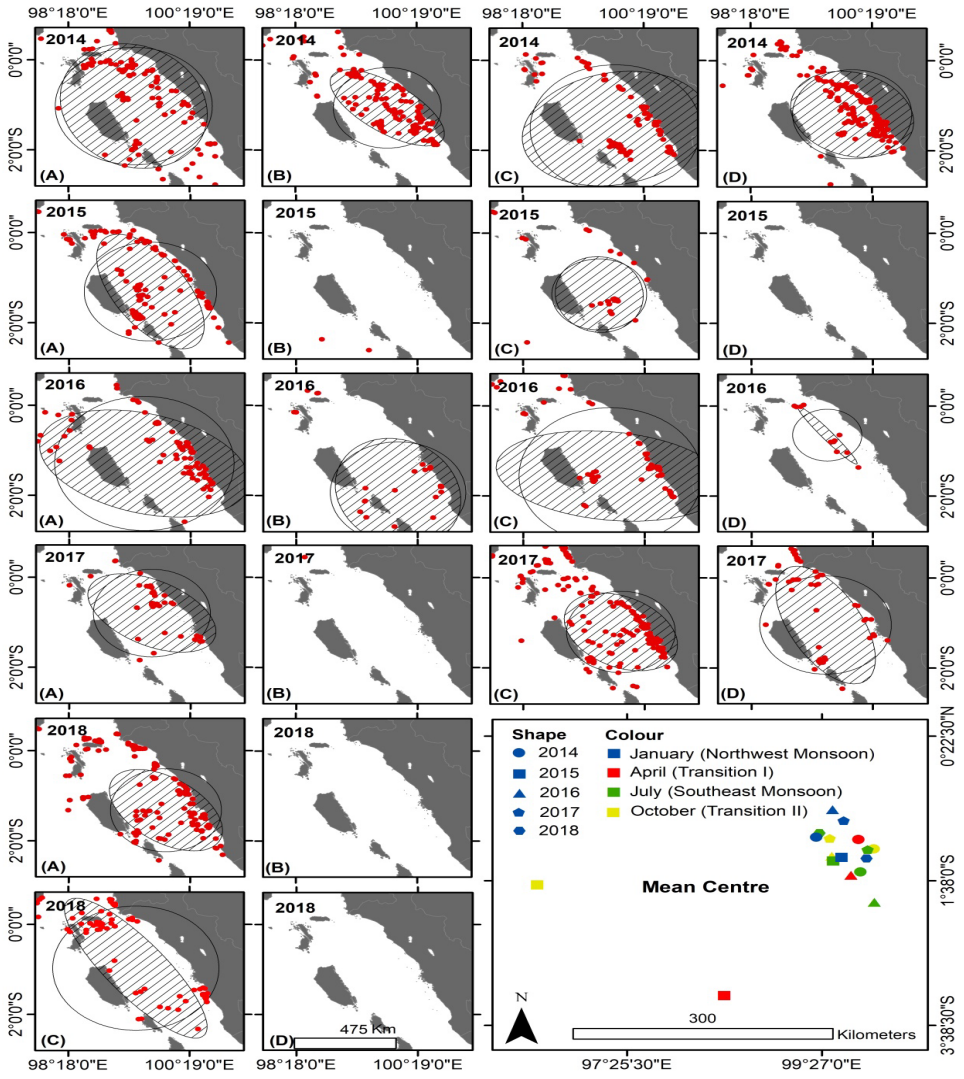

Figure 6. Map of VBD daily distribution per season from 2014 to 2018. Spatial dispersion (circles), directional dispersion, directional trends (ellipses), and mean centre (centre of fleet concentration from daily VBD per season). (A) Northwest monsoon, (B) Transition I, (C) Southeast monsoon, (D) Transition II

Environmental Parameters against Geographical Distribution

According to Siregar et al. (2018), the SST distribution in Indian Ocean is relatively warm with an average 28°C and cooler in southern part during the northwest monsoon so the north and south equatorial currents strengthen westward. SST gets warmer during transition I with value around 29°C and become colder in southeast monsoon because of the surface wind circulation pattern both in the northern hemisphere and southern hemisphere showing

regular patterns. During the transition II season, SST begins to get warmer due to weak wind circulation, the north equatorial current does not move yet causing colder SST at southern hemisphere of Indian Ocean. Chlorophyll-a concentration at western Sumatera waters consistently high at the west coast of Sumatera and at the southern area near Bota Island. Changes in current, wind, and atmospheric event influence the distribution of chlorophyll-a concentration at western Sumatera.

The variability of SST and chlorophyll-a concentration during different season influences the geographic distribution of light fishing fleet at west Sumatera waters. Figure 7 and 8 visually show that the geographical distribution of fishing fleets detected through VBD was very random spatially. In general, the VBD detection spread over a range of SST values between 27°C-32°C and chlorophyll-a concentration between 0.007 mg/m^3 to 0.42 mg/m^3. The lowest value of SST occurred in the northwest monsoon month in 2014 at a value of 27.96°C, and the highest occurred in the transition II in 2014 at the value of 31.99°C.

Meanwhile, the lowest value of chlorophyll-a concentration occurred in the southeast monsoon months and the first transition in 2014 at a value of 0.007 mg/m^3, with the highest value observed in the northwest monsoon in 2017 at 0.42 mg/m^3. Those parameters influenced fisheries distribution and determined fish habitat preferences. It is supported by the results of Nurdin et al. (2017) that mackerel preferred habitat at SST between 26.05°C - 31.97°C, with a chlorophyll-a concentration between 0.001 mg/m^3-0,1 mg/m^3. Siregar et al. (2018) also reported that range of SST preferences around 29°C – 29.5°C for yellow fin tuna species, chlorophyll-a concentration value in range between 0.15 – 0.25 mg m^{-3}. Harahap et al. (2018) also reported that variability of SST at range 29 – 31°C and chlorophyll-a concentration varied between 0.10 – 0.40 mg/m^3 were the main range related to the pelagic fish distribution at west Sumatera Waters. Chlorophyll-a concentration is a parameter that can indirectly determine water productivity and fish production. Thus, it is widely used in studies related to the determination of fish habitat preferences (Bertrand et al., 2002).

The geographical distribution pattern in the northwest monsoon was consistent with the directional dispersion (ellipse) and the standard dispersion (circles) patterns and had the same model and direction at x and y. From 2014 to 2017 for all seasons, the lowest distribution occurred in the southeast monsoon 2017 with an SST range between 29.22°C-31.52°C. Widest distribution occurred in the transition II 2015, where the VBD was detected in the Mentawai strait, and extended along the west coast of west Sumatra to the straits of Bota Island.

High SST was monitored at the northwest position of Bota Island and tended to be medium and low on the west coast of west Sumatra (Figure 7), where fishing activity was monitored to be dense from the results of boats detection. This spatial pattern was consistent with the distribution of chlorophyll-a, which was high on the coast (Figure 8). The highest

geographical distribution occurred in the second transitional season in 2015. The VBD points were detected spread and consistent towards the high distribution patterns of the SST in the west of Mentawai waters and on the west coast of West Sumatra. This distribution pattern was inconsistent with the spatial distribution patterns of the chlorophyll-a concentration that was high on the west coast to the south near the Pagai Islands.

Wyrtki (1961) stated that monsoons strongly influenced the circulation of the eastern Indian Ocean. The monsoon winds moving throughout the year affected the speed and direction of the sea surface, not apart from the waters of West Sumatra. Changes in wind direction occurred throughout the year would affect the course of the flow and movement of water masses in the Eastern Indian Ocean (EIO). It also influenced the variability of oceanographic parameters in the WSW, including sea surface temperature and chlorophyll-a concentration.

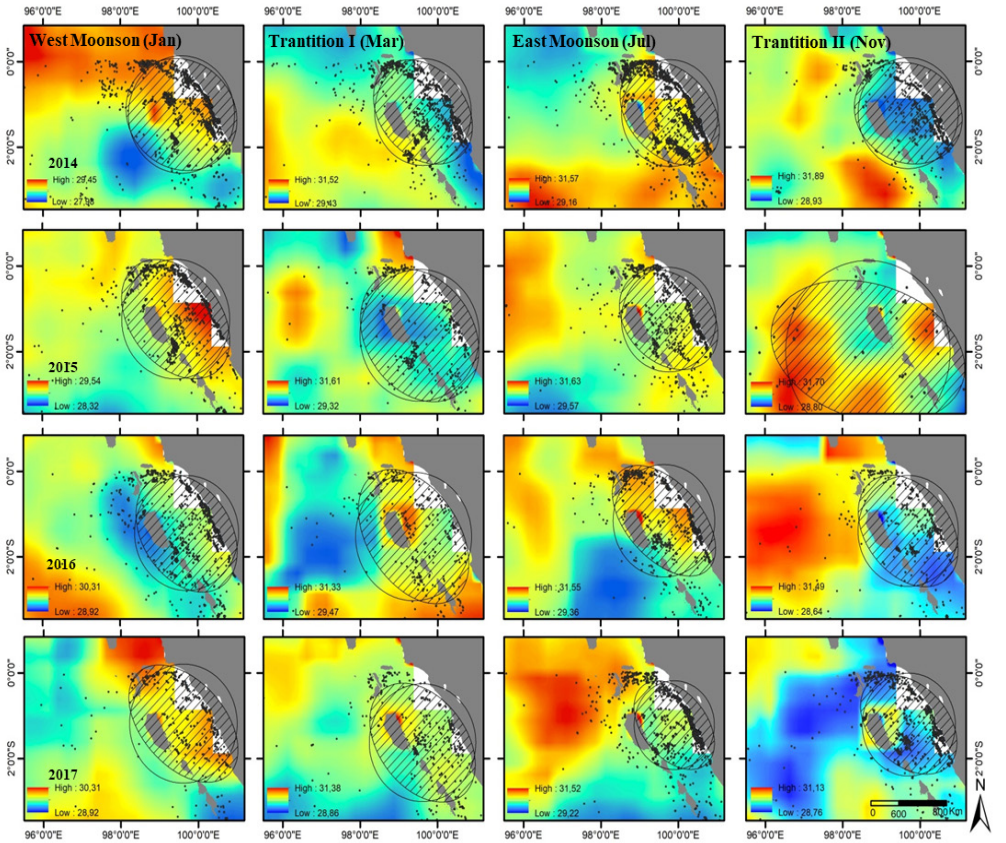

Figure 7. Monthly VBD distribution per season (northwest monsoon = January, transition I = April, southeast = July, transition II = November; consecutive left-to-right rows) in 2014-2017 (consecutive top-down column) on the spatial distribution of sea surface temperature (SST) in the West Sumatera Waters

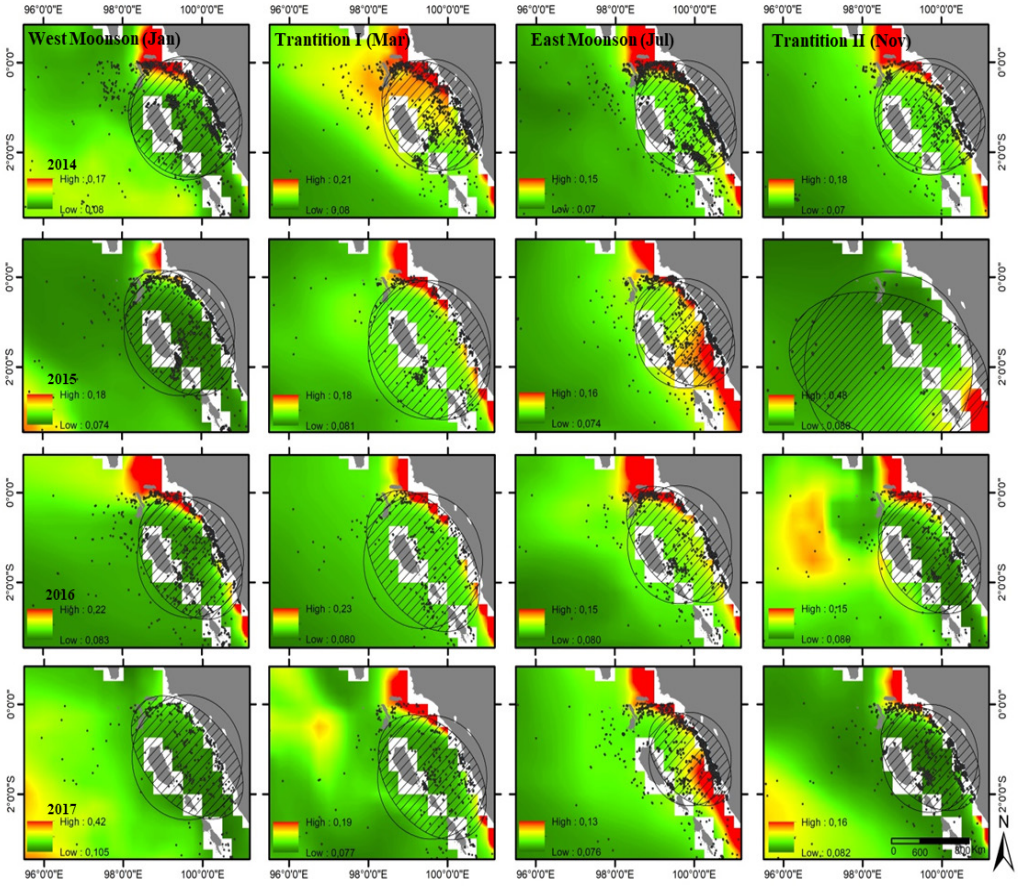

Figure 8. Monthly VBD distribution per season (northwest monsoon = January, transition I = April, southeast = July, transition II = November; consecutive left-to-right rows) in 2014-2017 (consecutive top-down column) on the spatial distribution of chlorophyll-a concentrations in West Sumatera Waters

CONCLUSION

The distribution of the VBD per pixel > 5 VBD/pixel was dominant in coastal waters, including the west coast of West Sumatra, the strait of the Bunga Sea and the coastal waters of Bota Island. The spatial pattern of the radiances showed that the value < 9.03 nW/cm^2/sr was dominantly spread out throughout the study area. The spatial models of the radiance values > 9.03 nW/cm^2/sr were dominant in waters near the coast and strait. This pattern was consistent with the spatial density, which was high in specific locations identified as CFA in this study. The largest CFA was recognized in CFA 2 with an area reaching 9813.74 km^2 in the waters of the West Sumatra coast. The CFA location extends from the south to the north near the straits of Bota Island. The smallest CFA was identified as CFA 16 covering

an area of 129.50 km^2 which was an area of north coast waters of northern Pagai Island or the waters of Pagai Island.

The highest spatial dispersion values were identified in the sample days in the northwest monsoon (2016) with a value of 168.94 km^2, indicates the wider distribution. The same results were also identified in the directional dispersion in the same year for *x* values of 204.92 km^2, but for *y* values, it did not linearly increase with the value of *x* and spatial dispersion. The directional trend of the distribution monitored from the estimation results showed the geographical orientation in ranging from 97.99^o to 171.48^o. The geographic distribution of light fishing fleets were in the SST between 27^{o}C-32^{o}C with chlorophyll-a between 0.007 mg/m^3 to 0.42 mg/m^3. The tendency of the geographical distribution of the fleet was dominant in coastal and strait waters.

ACKNOWLEDGMENT

The authors would like to express their gratitude to all the Bungus Fishing Port's staff for help in accessing the fishing logbook data. We also thank to Ministry of Research, Technology, and Higher Education of Indonesian Republic for funding this research in the Magister Thesis research scheme. This research was carried out using EU data Copernicus Marine Service Information. The authors also wish to express special thanks to colleagues in Marine Science and Technology Department, Marine GIS Laboratory, Marine Remote Sensing Laboratory, and Spatial Mapping and Modelling Laboratory, IPB University, for their suggestions and inputs in completing this research.

REFERENCES

Bertrand, A., Josse, E., Bach, P., Gros, P., & Dagorn, L. (2002). Hydrological and trophic characteristics of tuna habitat: consequences on tuna distribution and longline catchability. *Canadian Journal of Fisheries and Aquatic Sciences, 59*(6), 1002-1013.

Bertrand, A., Segura, M., Gutiérrez, M., & Vásquez, L. (2004). From small-scale habitat loopholes to decadal cycles: a habitat-based hypothesis explaining fluctuation in pelagic fish populations off Peru. *Fish and Fisheries, 5*(4), 296-316.

Booth, A. J. (2000). Incorporating the spatial component of fisheries data into stock assessment models. *ICES Journal of Marine Science*, *57*(4), 858-865.

Bungus Fishing Port. (2017). *Statistical report of bungus fishing port*. Padang, Indonesia.

Cabral, R. B., Gaines, S. D., Johnson, B. A., Bell, T. W., & White, C. (2016). Drivers of redistribution of fishing and non-fishing effort after the implementation of a marine protected area network. *Ecological Applications*, *27*(2), 416-428.

Close, C. H., & Hall, G. B. (2006). A GIS-based protocol for the collection and use of local knowledge in fisheries management planning. *Journal of Environmental Management*, *78*(4), 341-352.

Cozzolino, E., & Lasta, C. A. (2016). Use of VIIRS DNB satellite images to detect jigger ships involved in the Illex argentinus fishery. *Remote Sensing Applications: Society and Environment*, *4*, 167-178.

Davies, T. W., Duffy, J. P., Bennie, J., & Gaston, K. J. (2014). The nature, extent, and ecological implications of marine light pollution. *Frontiers in Ecology and the Environment*, *12*(6), 347-355.

Davies, T. W., Duffy, J. P., Bennie, J., & Gaston, K. J. (2016). Stemming the tide of light pollution encroaching into marine protected areas. *Conservation Letters*, *9*(3), 164-171.

Dineshbabu, A. P., Thomas, S., & Rohit, P. (2014). GIS-based spatial data analysis for marine fisheries management as a prerequisite for mariculture development. *Fishing Chimes, 33*(10-1), 91-93.

Elvidge, C. D., Baugh, K. E., Zhizhin, M., & Hsu, F. C. (2013). Why VIIRS data are superior to DMSP for mapping nighttime lights. *Proceedings of the Asia-Pacific Advanced Network, 35*(0), 62-69.

Elvidge, C. D., Ghosh, T., Baugh, K., Zhizhin, M., Hsu, F. C., Katada, N. S., … & Hung, B. Q. (2018). Rating the effectiveness of fishery closures with visible infrared imaging radiometer suite boat detection data. *Frontiers in Marine Science*, *5*(April), 1-15.

Elvidge, C. D., Zhizhin, M., Baugh, K., & Hsu, F. C. (2015). Automatic boat identification system for VIIRS low light imaging data. *Remote Sensing*, *7*(3), 3020-3036.

Elvidge, C., Zhizhin, M., Baugh, K., Hsu, F. C., & Ghosh, T. (2016). Methods for global survey of natural gas flaring from visible infrared imaging radiometer suite data. *Energies, 9*(1), 14-28.

Elvidge, C. D., Ziskin, D., Baugh, K. E., Tuttle, B. T., Ghosh, T., Pack, D. W., … & Zhizhin, M. (2009). A fifteen year record of global natural gas flaring derived from satellite data. *Energies*, *2*(3), 595-622.

Fischer, M. M., & Getis, A. (2010). *Handbook of Applied Spatial Analysis*. Heidelberg, Germany: Springer-Verlag

França, S., Vasconcelos, R. P., Fonseca, V. F., Tanner, S. E., Reis-Santos, P., Costa, M. J., & Cabral, H. N. (2012). Predicting fish community properties within estuaries: Influence of habitat type and other environmental features. *Estuarine, Coastal and Shelf Science*, *107*, 22-31.

Geronimo, R., Franklin, E., Brainard, R., Elvidge, C., Santos, M., Venegas, R., & Mora, C. (2018). Mapping fishing activities and suitable fishing grounds using nighttime satellite images and maximum entropy modelling. *Remote Sensing*, *10*(10), 1604-1626.

Girardin, R., Hamon, K. G., Pinnegar, J., Poos, J. J., Thébaud, O., Tidd, A., ... & Marchal, P. (2017). Thirty years of fleet dynamics modelling using discrete-choice models: What have we learned? *Fish and Fisheries, 18*(4), 638-655.

Harahap, M. A., Siregar, V. P., & Agus, S. A. (2018). *Analisis sebaran spasial dan temporal Ikan Pelagis berdasarkan parameter oseanografi di Perairan Sumatera Barat* [Analisys Spatial and Temporal Pelagic Fish Based on Oceanography Parameters in the Waters of West Sumatera] (Master Thesis). IPB University, Indonesia.

Hsu, F. C., Elvidge, C. D., Baugh, K., Zhizhin, M., Ghosh, T., Kroodsma, D., ... & Sudarja, Y. (2019). Cross-Matching VIIRS Boat Detections with Vessel Monitoring System Tracks in Indonesia. *Remote Sensing, 11*(9), 995-1020.

Jayaraman, J., George, G., Ambrose, T. V., & Manjeesh, R. (2013). Marine Geographic Information Systems and their Application in Fisheries Management. In S. K. Soam, P. D. Sreekanth & N. H. Rao (Eds.), *Geospatial technologies for natural resources management* (pp. 437-449). New Delhi, India: New India Publishing Agency.

Jennings, S., & Lee, J. (2012). Defining fishing grounds with vessel monitoring system data. *ICES Journal of Marine Science*, *69*(1), 51-63.

Kaschner, K., Watson, R., Trites, A. W., & Pauly, D. (2006). Mapping world-wide distributions of marine mammal species using a relative environmental suitability (RES) model. *Marine Ecology Progress Series, 316*, 285-310.

Kiyofuji, H., & Saitoh, S. I. (2004). Use of nighttime visible images to detect japanese common squid (*Todarodes pacificus*) fishing areas and potential migration routes in the sea of Japan. *Marine Ecology Progress Series*, *276*(1), 173-186.

Kroodsma, D. A., Mayorga, J., Hochberg, T., Miller, N. A., Boerder, K., Ferretti, F., ... & Woods, P. (2018). Tracking the global footprint of fisheries. *Science, 359*(6378), 904-908.

Lan, K. W., Evans, K., & Lee, M. A. (2013). Effects of climate variability on the distribution and fishing conditions of yellowfin tuna (*Thunnus albacares*) in the western Indian Ocean. *Climatic Change*, *119*(1), 63-77.

Lan, K. W., Shimada, T., Lee, M. A., Su, N. J., & Chang, Y. (2017). Using remote-sensing environmental and fishery data to map potential yellowfin tuna habitats in the Tropical Pacific Ocean. *Remote Sensing*, *9*(5), 1-14.

Lanz, E., López-martínez, J., Nevarez-martinez, M., & Dworak, J. A. (2009). Small pelagic fish catches in the Gulf of California associated with sea surface temperature and chlorophyll. *CalCOFI Reports, 50*, 134-146.

Lumban-Gaol, J., Leben, R. R., Vignudelli, S., Mahapatra, K., Okada, Y., Nababan, B., … & Syahdan, M. (2015). Variability of satellite-derived sea surface height anomaly, and its relationship with Bigeye tuna (*Thunnus obesus*) catch in the Eastern Indian Ocean. *European Journal of Remote Sensing*, *48*(1), 465-477.

Miller, S. D., Straka, W., Mills, S. P., Elvidge, C. D., Lee, T. F., Solbrig, J., … & Weiss, S. C. (2013). Illuminating the capabilities of the suomi national polar-orbiting partnership (NPP) visible infrared imaging radiometer suite (VIIRS) day/night band. *Remote Sensing*, *5*(12), 6717-6766.

Mulyadi, R. A., Brown, A., & Rengi, P. (2015). Study technology hand line fishing in Port Bungus West Sumatra. *Online Journal*, *2*, 1-13.

Nurdin, S., Mustapha, A., Chan, Y., & Lihan, T. (2010, July 26-28). Mapping of potential fishing grounds of Rastrelliger kanagurta (Cuvier, 1817) using satellite images. In *Proceedings of Map Asia & ISG* (pp. 1-9). Kuala Lumpur, Malaysia.

Nurdin, S., Mustapha, A., Lihan, T., & Ghaffar, A. A. (2015). Determination of potential fishing grounds of Rastrelliger kanagurta using satellite remote sensing and GIS technique. *Sains Malaysiana*, *44*(2), 225-232.

Nurdin, S., Mustapha, M. A., Lihan, T., & Zainuddin, M. (2017). Applicability of remote sensing oceanographic data in the detection of potential fishing grounds of Rastrelliger Kanagurta in The Archipelagic Waters of Spermonde, Indonesia. *Fisheries Research*, *196*(July), 1-12.

Palenzuela, J., Iglesias, G., & Vilas, L. (2004). Pelagic fisheries study using GIS and remote sensing imagery in Galicia (Spain). *ICES CM*, *44*, 1-5.

Parnell, P. E., Dayton, P. K., Fisher, R. A., Loarie, C. C., & Darrow, R. D. (2010). Spatial patterns of fishing effort off San Diego: implications for zonal management and ecosystem function. *Ecological Applications, 20*(8), 2203-2222.

Perzia, P., Battaglia, P., Consoli, P., Andaloro, F., & Romeo, T. (2016). Swordfish monitoring by a GIS-based spatial and temporal distribution analysis on harpoon fishery data: A case of study in The Central Mediterranean Sea. *Fisheries Research*, *183*(2016), 424-434.

Pierce, G. J., Wang, J., Zheng, X., Bellido, J. M., Boyle, P. R., Denis, V., & Robin, J. (2002). A cephalopod fishery GIS for the Northeast Atlantic: Development and application. *International Journal of Geographical Information Science, 15*(8), 1-22.

Riolo, F. (2006). A geographic information system for fisheries management in American Samoa. *Environmental Modelling and Software*, *21*(7), 1025-1041.

Saitoh, S., Fukaya, A., Saitoh, K., Semedi, B., & Mugo, R. (2010). Estimation of number of pacific saury fishing vessels using night-time visible images. *International Archives of the Photogrammetry, Remote Sensing and Spatial Information Science, 38*, 1013-1016.

Saraux, C., Fromentin, J. M., Bigot, J. L., Bourdeix, J. H., Morfin, M., Roos, D., … & Bez, N. (2014). Spatial structure and distribution of small pelagic fish in the northwestern mediterranean sea. *PLoS ONE*, *9*(11), 1-12.

Setiawati, M., & Tanaka, T. (2017). Utilization of scatterplot smoothers to understand the environmental preference of Bigeye Tuna in the Southern Waters off Java-Bali: Satellite remote sensing approach. *Fishes*, *2*(1), 1-16.

Siregar, E. S., Siregar, V. P., & Agus, S. A. (2018). *Prediksi zona potensi penangkapan Ikan Tuna Sirip Kuning (Thunnus Albacares) menggunakan model gam di Perairan Sumatera Barat* [Prediction of Potential Fishing Zones for Yellowfin Tuna (*Thunnus albacares*) Using GAM Models in West-Sumatera Waters] (Master Thesis). IPB University, Indonesia.

Stewart, K. R., Lewison, R. L., Dunn, D. C., Bjorkland, R. H., Kelez, S., Halpin, P. N., & Crowder, L. B. (2010). Characterizing fishing effort and spatial extent of coastal fisheries. *PLoS ONE*, *5*(12), 1-8.

Straka, W. C., Seaman, C. J., Baugh, K., Cole, K., Stevens, E., & Miller, S. D. (2015). Utilization of the suomi national polar-orbiting partnership (SNPP) visible infrared imaging radiometer suite (VIIRS) day/night band for arctic ship tracking and fisheries management. *Remote Sensing*, *7*(1), 971-989.

Syah, A. F., Saitoh, S. I., Alabia, I. D., & Hirawake, T. (2016). Predicting potential fishing zones for pacific saury (*Cololabis saira*) with maximum entropy models and remotely sensed data. *Fishery Bulletin*, *114*(3), 330-342.

Tidd, A., Brouwer, S., & Pilling, G. (2017). Shooting fish in a barrel? Assessing fisher-driven changes in catchability within tropical tuna purse seine fleets. *Fish and Fisheries*, *18*(5), 808-820.

Wyrtki, K. (1961). *Physical oceanography of the Southeast Asian waters.* San Diego, California: Scripps Institution of Oceanography.

Zainuddin, M. (2011). Skipjack tuna in relation to sea surface temperature and chlorophyll-a concentration of bone bay using remotely sensed satellite data. *Jurnal Ilmu Dan Teknologi Kelautan Tropis*, *3*(1), 82-90.

Zainuddin, M., & Saitoh, K. (2008). Albacore (*Thunnus alalunga*) fishing ground in relation to oceanographic conditions in the western North Pacific Ocean using remotely sensed satellite data. *Fisheries Oceanography, 17*(2), 61-73.

Zhang, X., Saitoh, S. I., & Hirawake, T. (2017). Predicting potential fishing zones of Japanese common squid (*Todarodes pacificus*) using remotely sensed images in coastal waters of south-western Hokkaido, Japan. *International Journal of Remote Sensing*, *38*(21), 6129-6146.